# Cerebral Hemodynamics on MR Perfusion Images before and after Bypass Surgery in Patients with Giant Intracranial Aneurysms

Francesca Caramia, Antonio Santoro, Patrizia Pantano, Emiliano Passacantilli, Giulio Guidetti, Alberto Pierallini, Luigi Maria Fantozzi, Gian Paolo Cantore and Luigi Bozzao

*AJNR Am J Neuroradiol* 2001, 22 (9) 1704-1710
http://www.ajnr.org/content/22/9/1704

*AJNR Am J Neuroradiol* 22:1704–1710, October 2001

# Cerebral Hemodynamics on MR Perfusion Images before and after Bypass Surgery in Patients with Giant Intracranial Aneurysms

Francesca Caramia, Antonio Santoro, Patrizia Pantano, Emiliano Passacantilli, Giulio Guidetti, Alberto Pierallini, Luigi Maria Fantozzi, Gian Paolo Cantore, and Luigi Bozzao

***BACKGROUND AND PURPOSE:*** **Preoperative assessment of the anatomy and dynamics of cerebral circulation for patients with giant intracranial aneurysm can improve both outcome prediction and therapeutic approach. The aim of our study was to use perfusion MR imaging to evaluate cerebral hemodynamics in such patients before and after extraintracranial high-flow bypass surgery.**

***METHODS:*** **Five patients with a giant aneurysm of the intracranial internal carotid artery underwent MR studies before, 1 week after, and 1 month after high-flow bypass surgery. We performed MR and digital subtraction angiography, and conventional and functional MR sequences (diffusion and perfusion). Surgery consisted of middle cerebral artery (MCA)–internal carotid artery bypass with saphenous vein grafts (n = 4) or MCA–external carotid artery bypass (n = 1).**

***RESULTS:*** **In four patients, MR perfusion study showed impaired hemodynamics in the vascular territory supplied by the MCA of the aneurysm side, characterized by significantly reduced mean cerebral blood flow (CBF), whereas mean transit time (MTT) and regional cerebral blood volume (rCBV) were either preserved, reduced, or increased. After surgery, angiography showed good canalization of the bypass graft. MR perfusion data obtained after surgery showed improved cerebral hemodynamics in all cases, with a return of CBF index (CBFi), MTT, and rCBV to nearly normal values.**

***CONCLUSION:*** **Increased MTT with increased or preserved rCBV can be interpreted as a compensatory vasodilatory response to reduced perfusion pressure, presumably from compression and disturbed flow in the giant aneurysmal sac. When maximal vasodilation has occurred, however, the brain can no longer compensate for diminished perfusion by vasodilation, and rCBV and CBFi diminish. Bypass surgery improves hemodynamics, increasing perfusion pressure and, thus, CBFi. Perfusion MR imaging can be used to evaluate cerebral hemodynamics in patients with intracranial giant aneurysm.**

Untreated giant intracranial aneurysms are a serious disorder and have a dismal natural history as a result of hemorrhage, cerebral compression, and ischemia (1, 2). Aneurysms can cause ischemic symptoms by harboring thrombi that embolize distally (3). Propagation of thrombus could be another explanation for ischemia in thrombosed aneurysms (4). Patients with giant aneurysms also may develop cerebral ischemia because the enlarging aneurysm can compress or stretch the parent artery or neighboring vessels (5–7).

The poor prognosis of patients with giant aneurysms warrants aggressive treatment. Surgical treatment of this condition—clipping or bypass surgery—carries considerable risks as well as potential benefits. The treatment of choice for intracranial aneurysms is to exclude the aneurysmal sac from the circulation, while preserving the parent arteries by surgical intervention (8) or endovascular technique (9). Some cerebral aneurysms are not amenable to treatment by traditional techniques because of their anatomic conformation and location. The available therapeutic options for such lesions include a direct surgical approach (8); surgical or

Received October 23, 2000; accepted after revision May 7, 2001.

From the Neuroradiology (F.C., P.P., G.G., A.P., L.M.F., L.B.) and Neurosurgery Sections (A.S., E.P., G.P.C.), I and II (L.M.F.) School of Medicine, University of Rome ''La Sapienza''; and IRCCS Neuromed (L.B.), Pozzilli, Italy.

Address reprint requests to Francesca Caramia, Neuroradiology Section, Department of Neurological Sciences, University of Rome ''La Sapienza'', Viale dell'Universitá 30, 00185 Rome, Italy.

**TABLE 1: Characteristics of aneurysms and surgical procedures**

| Patient No. | Sex | Age (y) | Site of Aneurysm | Total Size (mm) | Patent Size (mm) | Operation: Anastomosis |
|---|---|---|---|---|---|---|
| 1 | Male | 25 | Left ICA-ophthalmic artery | 20 × 22 × 18 | 20 × 22 × 18 | ECA-MCA |
| 2 | Female | 41 | Left ICA-posterior communicating artery | 30 × 28 × 24 | 30 × 28 × 24 | ICA-MCA |
| 3 | Female | 68 | Left ICA | 32 × 36 × 36 | 32 × 36 × 36 | ICA-MCA |
| 4 | Male | 43 | Right ICA | 42 × 35 × 42 | 30 × 24 × 36 | ICA-MCA |
| 5 | Male | 46 | Left ICA-ophthalmic artery | 70 × 40 × 48 | 32 × 28 × 42 | ICA-MCA |

endovascular occlusion of the internal carotid artery (ICA) in the neck, in selected cases combined with a bypass graft from the superficial temporal artery to the middle cerebral artery (MCA); a long saphenous vein interposition graft from the intracranial circulation to the carotid artery in the neck; or a short graft from the intrapetrous artery to the supraclinoid carotid artery (10, 11).

Preoperative assessment of the anatomy and dynamics of cerebral circulation is essential, to avoid distal cerebral ischemia (12–16) and to guide the therapeutic choice. Perfusion MR imaging represents a noninvasive technique to evaluate cerebral hemodynamics (17–26). The aim of our study was to use perfusion MR imaging to study cerebral hemodynamics in patients with giant intracranial aneurysms before and after bypass surgery. In particular, we wished to evaluate the presence of impaired perfusion, even in the absence of ischemic brain damage and to investigate the effect of bypass surgery on cerebral hemodynamics 1 week and 1 month after bypass surgery.

## Methods

### *Patients*

Five adult patients with a unilateral, unruptured, giant cerebral aneurysm were evaluated after admission to our department between April 1999 and April 2000. There were three men and two women. Ages ranged from 25 to 68 years old (mean ± SD, 45 ± 15 years). The distribution of aneurysm site was as follows: ICA, two cases; ICA−ophthalmic artery, two cases; and ICA−posterior communicating artery, one case (Table 1). Symptoms at presentation included headache in two patients and headache and cranial nerve deficit in three patients.

### *Imaging*

All patients underwent digital subtraction angiography (DSA) before and after surgery. Four patients tolerated a balloon occlusion test before surgery; one patient failed the test (patient 1). MR study was performed in all patients before surgery, 1 week after surgery, and 1 month after surgery. In one case, the 1-week MR study was not available for technical reasons, and in another, the 1-month MR study was not performed because the patient had been transferred to another institution.

All MR images were obtained on a clinical 1.5-T unit (Gyroscan NT 2000; Philips, Best, The Netherlands) by use of a standard quadrature head coil. MR imaging began with a T1-weighted localizer on three orthogonal planes, followed by T2- and T1-weighted sequences before and after injection of a contrast agent (for T2, 17/110/3500 [$TE_1$/$TE_2$/TR]; for T1, 14/560 [TE/TR]; slice thickness, 5 mm; gap, 1 mm; field of view [FOV], 230; number of signals averaged (NSA), 1; and matrix, 256 × 512), MR angiography of the intracranial vessels (3D time of flight; 3.5/30 [TE/TR]; flip angle, 20°; FOV, 220; NSA, 1; and matrix, 256 × 512), diffusion-weighted sequences (single-shot echo-planar imaging [EPI] sequence; EPI factor, 63; 110/3600 [TE/TR]; slice thickness, 6 mm; gap, 1 mm; FOV, 230; NSA, 1; matrix, 128 × 256), and perfusion MR imaging. Conventional T2- and T1-weighted images, diffusion-weighted (DW) images, and apparent diffusion coefficient maps were reviewed by two neuroradiologists (F.C., A.P.). Aneurysm size and presence of thrombosis were assessed on T2-weighted conventional images and on DSA images. Aneurysm size was estimated by calculating the anteroposterior diameter, lateral maximal diameter, and craniocaudal diameter; each diameter was obtained by multiplying the section thickness (and gap) by the number of sections where the aneurysm was present.

The perfusion MR studies were performed on 12 axial sections, which were selected to include most of the MCA territory. Perfusion MR imaging was performed on 7-mm sections (gap, 0) using a multishot EPI gradient-echo sequence with 440/30/45° (TR/TE/flip angle). The other imaging parameters included an FOV of 240, EPI factor of 11, NSA of 1, and matrix of 80 × 128. The imaging time per image was 2.2 seconds. These images were acquired sequentially 40 times, yielding a total imaging time of about 1.5 minutes. Perfusion MR imaging was performed with the patients' heads in the dimly lit MR unit; no visually salient features were present during the imaging. After the first 10 MR images were acquired as baseline images, 20 mL of gadolinium contrast agent (Magnevist; Schering Diagnostics, Berlin, Germany) was manually injected as an intravenous bolus. The 40 sequential images were analyzed at the MR workstation using dedicated software (Philips Packman). For each pixel, the measured time course of the MR imaging signal intensity was fitted to a modified gamma function (27–30). The fit yielded the mean transit time (MTT), calculated as the first moment of the curve and the area under the curve (which is proportional to the regional cerebral blood volume, rCBV). With these two variables, an index of cerebral blood flow (CBFi) was calculated according to the equation: CBFi = rCBV/MTT. The time to the peak signal change (TTP) also was calculated as a temporal variable related to the transit time (20). The resulting image was displayed as rCBV, CBFi, MTT, and TTP maps (Fig 1A and B) by using gray scale.

Bilateral and symmetrical regions of interest (ROIs) were arbitrarily chosen on the MCA territory, not including areas of T2 hyperintensity and artifacts due to metallic implants (if present); three ROIs were outlined on each side on the frontal, frontoparietal, and parietal lobes. Asymmetry indices were calculated for each hemodynamic variable (rCBV, CBFi, and MTT) by dividing the values for the ROI on the side of the aneurysm by the values obtained on the contralateral side.

### *Surgery*

Before surgery, all patients consented to craniotomy and bypass surgery, about which our staff neurosurgeons informed them in detail. A frontotemporal approach was used in all cases. Bypass with a long saphenous vein graft was established

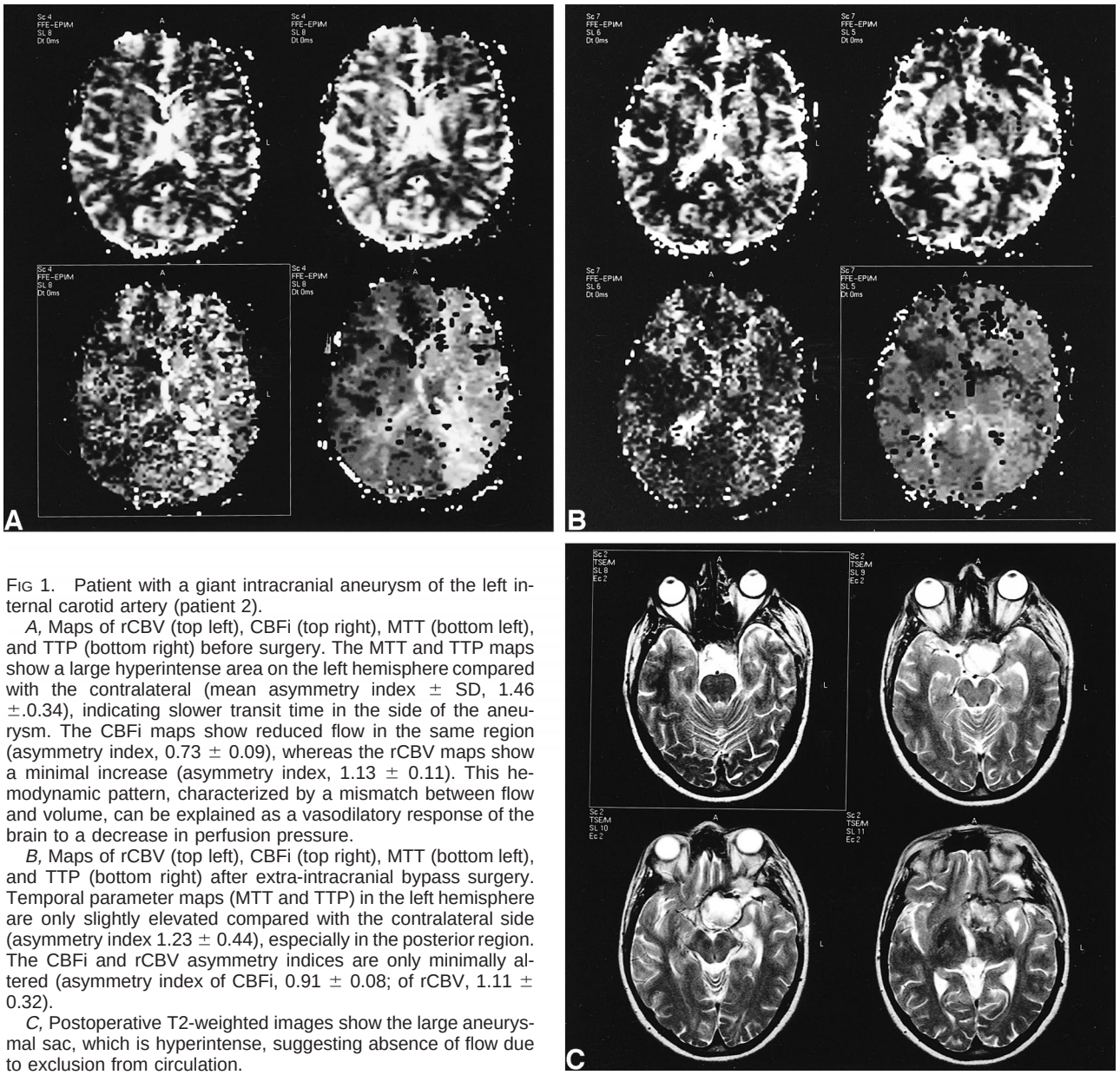

FIG 1. Patient with a giant intracranial aneurysm of the left internal carotid artery (patient 2).

*A,* Maps of rCBV (top left), CBFi (top right), MTT (bottom left), and TTP (bottom right) before surgery. The MTT and TTP maps show a large hyperintense area on the left hemisphere compared with the contralateral (mean asymmetry index ± SD, 1.46 ±.0.34), indicating slower transit time in the side of the aneurysm. The CBFi maps show reduced flow in the same region (asymmetry index, 0.73 ± 0.09), whereas the rCBV maps show a minimal increase (asymmetry index, 1.13 ± 0.11). This hemodynamic pattern, characterized by a mismatch between flow and volume, can be explained as a vasodilatory response of the brain to a decrease in perfusion pressure.

*B,* Maps of rCBV (top left), CBFi (top right), MTT (bottom left), and TTP (bottom right) after extra-intracranial bypass surgery. Temporal parameter maps (MTT and TTP) in the left hemisphere are only slightly elevated compared with the contralateral side (asymmetry index 1.23 ± 0.44), especially in the posterior region. The CBFi and rCBV asymmetry indices are only minimally altered (asymmetry index of CBFi, 0.91 ± 0.08; of rCBV, 1.11 ± 0.32).

*C,* Postoperative T2-weighted images show the large aneurysmal sac, which is hyperintense, suggesting absence of flow due to exclusion from circulation.

between the ICA and MCA in four cases and between the external carotid artery (ECA) and MCA in one case. After careful monitoring of bypass patency by either intraoperative angiography or Doppler sonography, the ICA was clipped beyond the intracavernous tract. In one case, the inferior anastomosis was established with the ECA, and the ICA was closed at the neck. During surgery, the duration of occlusion for the temporal branches of the MCA ranged from 35 to 48 minutes (mean, 40.6 ± 4.9 min).

### *Statistical Analysis*

Statistical analysis was performed by using a two-tailed, paired, Student's *t* test between values calculated in the affected hemisphere and the contralateral side and between asymmetry indices obtained on different studies (the asymmetry indices of CBFi, rCBV, and MTT calculated before surgery vs those at the 1-week follow-up study, and before surgery vs 1 month after surgery).

## Results

When considering only the patent lumen, the maximum diameter of the aneurysms ranged from 22 to 42 mm (mean, 33.2 ± 7.5 mm); when including the thrombosed regions, the maximum diameter ranged from 22 to 70 mm (mean, 40 ± 18 mm) (Table 1).

On conventional T2-weighted MR images obtained before surgery, two patients showed hyperintense areas of brain tissue around the aneurysm, interpreted as ischemic tissue damage and edema (patients 4 and 5) (Table 2). On the postoperative images, the hyperintense area was enlarged in patient 4 and reduced in patient 5. Three patients showed new hyperintense areas on T2-weighted MR images obtained after surgery (patients 1, 2,

**TABLE 2: MR findings on T2-weighted images and on DW images before and after bypass surgery**

| Time | T2 Abnormalities | DW Abnormalities |
|---|---|---|
| Patient 1 | | |
| Before surgery | None | None |
| 1 week after surgery | Left insular cortex, caudate nucleus, centrum semiovalis | Left insular cortex, caudate nucleus, centrum semiovalis |
| 1 month after surgery | — | — |
| Patient 2 | | |
| Before surgery | None | None |
| 1 week after surgery | Left basal ganglia | None |
| 1 month after surgery | Unchanged | None |
| Patient 3 | | |
| Before surgery | None | None |
| 1 week after surgery | — | — |
| 1 month after surgery | Small left frontotemporal white matter | None |
| Patient 4 | | |
| Before surgery | Right frontotemporal white matter | None |
| 1 week after surgery | Larger, same location | Right frontotemporal white matter |
| 1 month after surgery | Unchanged | Faint, same location |
| Patient 5 | | |
| Before surgery | Left frontotemporal and parietal white matter, basal ganglia | None |
| 1 week after surgery | Smaller, same location | None |
| 1 month after surgery | Unchanged | None |

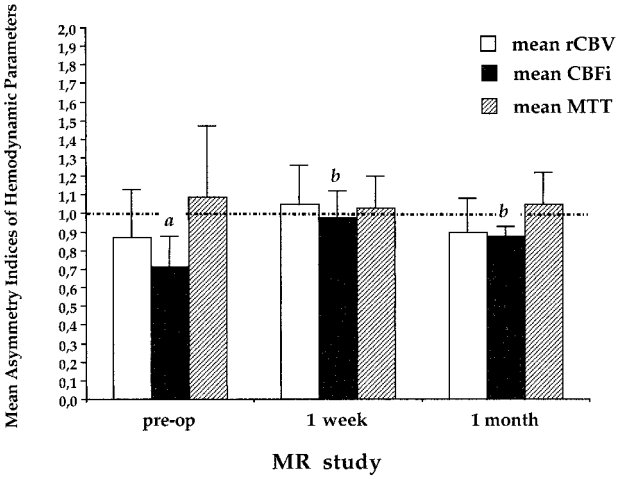


FIG 2. Mean asymmetry indices (±SD) for rCBV, CBFi, and MTT from MR studies performed in five patients before, 1 week after, and 1 month after bypass surgery. Bars represent the mean values of each of the three variables calculated in all patients: *a* indicates significantly lower values on the affected side than on the contralateral side ($P = .0001$); *b* indicates postoperative asymmetry indices significantly higher than the preoperative values ($P < .05$).

and 3), which were thought to be due to contusions or infarctions. All patients showed fluid collections in the subdural spaces on MR scans obtained 1 week after surgery.

Figure 2 shows the pre- and postoperative data for the five patients. Before surgery, the hemodynamic disturbances consisted of a significant decrease in CBFi on the affected side compared with the contralateral side (mean asymmetry index, 0.71 ± 0.17; $P = .0001$), an increase in MTT (mean asymmetry index, 1.09 ± 0.32), and a slight decrease in rCBV (mean asymmetry index, 0.87 ± 0.2).

One week after surgery, CBFi values were close to normal (mean asymmetry index, 0.98 ± 0.14) and showed a slight and nonsignificant decrease after 1 month (mean asymmetry index, 0.88 ± 0.05). CBFi values 1 week and 1 month after surgery both were significantly increased ($P = .04$ and $P = .009$, respectively) compared with preoperative values (Fig 2).

The five patients showed different perfusion patterns, however (Fig 3) (Table 3). Hemodynamic disturbance was more severe in the two patients who had tissue damage on the conventional MR images before surgery (patients 4 and 5). In both cases, the aneurysmal sac was partially thrombosed, and both showed an increase in CBFi on follow-up studies (Table 3). Of the three patients without alterations on the T2-weighted MR images obtained before surgery (patients 1, 2, and 3), two had substantial increases in MTT (mean asymmetry index values, 1.28 ± 0.1 and 1.46 ± 0.3), slight rCBV increases, and decreases in CBFi before surgery. All three variables returned to values close to those of the contralateral side after surgery. CBFi increased at the 1-week follow-up studies in these two patients and remained higher than the preoperative level at the 1-month study. Only one patient (patient 1) had normal hemodynamic values both before and after surgery.

## Discussion

The main finding of this study is that perfusion MR imaging can show perturbation of cerebral he-

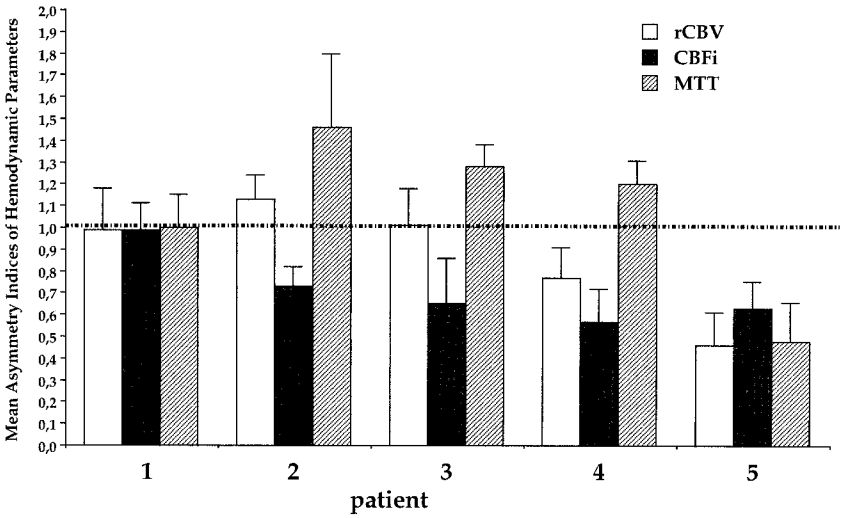


FIG 3. Mean asymmetry indices (± SD) for rCBV, CBFi, and MTT in five patients with intracranial aneurysm before surgery. Bars represent the mean asymmetry index of each of the three variables calculated in single patients.

**TABLE 3: Mean asymmetry indices (±SD) in the MCA territory before and after bypass surgery**

| Time | rCBV | CBFi | MTT |
|---|---|---|---|
| Patient 1 | | | |
| Before surgery | 0.99 ± 0.19 | 0.99 ± 0.12 | 1.00 ± 0.15 |
| 1 week after surgery | 1.18 ± 0.08 | 1.08 ± 0.09 | 1.15 ± 0.11 |
| 1 month after surgery | — | — | — |
| Patient 2 | | | |
| Before surgery | 1.13 ± 0.11 | 0.73 ± 0.09 | 1.46 ± 0.34 |
| 1 week after surgery | 1.08 ± 0.11 | 1.10 ± 0.10 | 0.88 ± 0.03 |
| 1 month after surgery | 1.11 ± 0.32 | 0.91 ± 0.08 | 1.23 ± 0.44 |
| Patient 3 | | | |
| Before surgery | 1.01 ± 0.17 | 0.65 ± 0.21 | 1.28 ± 0.10 |
| 1 week after surgery | — | — | — |
| 1 month after surgery | 1.00 ± 0.37 | 0.91 ± 0.11 | 1.13 ± 0.64 |
| Patient 4 | | | |
| Before surgery | 0.77 ± 0.14 | 0.57 ± 0.15 | 1.20 ± 0.11 |
| 1 week after surgery | 1.21 ± 0.19 | 0.94 ± 0.07 | 1.21 ± 0.04 |
| 1 month after surgery | 0.75 ± 0.07 | 0.91 ± 0.30 | 0.83 ± 0.08 |
| Patient 5 | | | |
| Before surgery | 0.46 ± 0.15 | 0.63 ± 0.12 | 0.48 ± 0.18 |
| 1 week after surgery | 0.74 ± 0.09 | 0.80 ± 0.17 | 0.91 ± 0.11 |
| 1 month after surgery | 0.74 ± 0.13 | 0.80 ± 0.17 | 1.00 ± 0.05 |

modynamics in patients harboring an unruptured giant cerebral aneurysm. MR perfusion measurements showed reduced mean CBFi, slightly decreased rCBV, and increased MTT in the MCA territory ipsilateral to a giant internal carotid aneurysm.

These results agree with a recent CBF single-photon emission CT study, which used $^{99m}$Tc-ethyl cysteinate dimer to study patients with unruptured cerebral aneurysms. This study showed a reduced CBF in 30% of the patients (31).

In our study, a spectrum of hemodynamic patterns was found in individual patients, ranging from normal perfusion (patient 1), to an increased MTT with a slightly decreased CBFi (patients 2 and 3), to similarly reduced blood volume and flow (patients 4 and 5). Conventional MR imaging also showed heterogeneous findings, consisting of no apparent tissue damage in three patients (patients 1–3) and a lesion of variable extent in the affected hemisphere in the other two (patients 4 and 5). Only one patient (patient 1) had neither hemodynamic alterations nor ischemic lesions before surgery; this patient had the smallest aneurysm in our series.

In two patients (patients 2 and 3), we observed increased or preserved rCBV, increased MTT, and slightly decreased CBFi. The MTT prolongation and the CBV/CBF mismatch could be explained by a compensatory vasodilatory response to reduced cerebral perfusion pressure. This mechanism aims to maintain a blood supply adequate to metabolic demand, as shown by the absence of ischemic damage in these two patients. Such a hemodynamic response also has been observed in patients with carotid stenosis (26, 32, 33).

Two other patients (patients 4 and 5) showed parallel decreases in rCBV and CBFi. This hemodynamic pattern identifies a situation where the compensatory vasodilation mechanism is exhausted, and further decreases in cerebral perfusion pressure translate into parallel decreases in both blood volume and flow (34). This critical hemodynamic condition may have contributed to the tissue damage shown as hyperintense areas around the aneurysm and within the MCA territory on T2-weighted images in these two patients.

Patients with giant aneurysms may develop cerebral ischemia due to various pathophysiological mechanisms, including stretching or compression of the parent artery by the enlarging aneurysm (5–7). Experimental as well as human studies have shown that flow in large aneurysms is complicated by blood stagnation, increased blood viscosity, and slow flow (5, 35–37). This alteration of flow dynamics within the large aneurysmal sac could contribute to local changes in perfusion pressure. Furthermore, in the two patients who showed tissue

damage on T2-weighted images (patients 4 and 5), the aneurysmal sac was partially thrombosed. We cannot exclude that thrombosis was responsible for ischemia in these cases by embolization (3, 5).

All patients underwent revascularization, establishing the bypass between the ECA and MCA in the one patient who failed the balloon occlusion test, and between the ICA and MCA in the other four patients. Because no carotid occlusion test can exclude the risk of late complications after ICA sacrifice (38–41), our group, in agreement with others, believes that cerebral revascularization is indicated even for patients with adequate collateral circulation, particularly those with long life expectancy.

After high-flow bypass surgery, cerebral hemodynamics improved on the side of the aneurysm in all cases. The persistence of perfusion changes over the 1-month observation period suggests that the CBFi increase is a stable phenomenon and does not result exclusively from transient hyperemic changes after reperfusion.

The improvement of cerebral hemodynamics we observed refers to regions within the vascular territory supplied by the affected artery but outside the area of tissue damage, if present. This indicates that a large amount of viable but hemodynamically compromised tissue may benefit from bypass surgery.

Our study adds to several reports investigating alternative techniques to evaluate cerebral hemodynamics before bypass surgery (12–16). Perfusion MR imaging is noninvasive and easily identifies patients with altered hemodynamics. The presence of a mismatch between flow and volume in certain patients indicates a critical condition in which the tissue is still viable but at risk of ischemia (23, 34, 42). Parallel decreases in both volume and flow indicate a more severe hemodynamic condition in which the perfusion reserve is exhausted and the risk of infarction is real, as documented by the tissue damage observed in the two patients with such a perfusion pattern in this study. Perfusion MR imaging can provide useful preoperative information by identifying patients at risk of ischemia. This risk should be taken into account, along with that of bleeding, in patients with giant unruptured aneurysms, as an indication to surgical treatment.

## Conclusion

Patients harboring giant cerebral aneurysms may have altered cerebral hemodynamics even in the absence of tissue damage and the presence of collateral circulation. Perfusion MR imaging can identify the hemodynamic consequences of a carotid artery aneurysm and monitor its evolution. The hemodynamic evaluation of patients with giant aneurysms before and after surgery may improve the prediction of outcomes, can help select the optimal surgical procedure, and can allow noninvasive, long-term patient monitoring.

## References


1. Raaymakers TWM, Rinkel GJE, Limburg M, Algra A. **Mortality and morbidity of surgery for unruptured intracranial aneurysms: a meta-analysis.** *Stroke* 1998;29:1531–1538
2. Lawton MT, Spetzler RF. **Surgical strategies for giant intracranial aneurysms.** *Acta Neurochir Suppl (Wien)* 1999;72:141–156
3. Qureshi AI, Mohammad Y, Yahia AM, et al. **Ischemic events associated with unruptured intracranial aneurysms: multicenter clinical study and review of the literature.** *Neurosurgery* 2000;46:282–290
4. Brownlee RD, Tranmer BI, Sevick RJ, Karmy G, Curry BJ. **Spontaneous thrombosis of an unruptured anterior communicating artery aneurysm: an unusual cause of ischemic stroke.** *Stroke* 1995;26:1945–1949
5. Whittle IR, Dorsch NW, Besser M. **Spontaneous thrombosis in giant intracranial aneurysms.** *J Neurol Neurosurg Psychiatry* 1982;45:1040–1047
6. Segal HD, McLaurin RL. **Giant serpentine aneurysm: report of two cases.** *J Neurosurg* 1977;46:115–120
7. Sato K, Fujiwara AS, Yoshimoto T, Onuma T. **Two cases of spontaneous internal carotid artery occlusion due to giant intracranial carotid artery aneurysm.** *Stroke* 1990;21:1506–1509
8. Spetzler RF, Carter LP. **Revascularization and aneurysm surgery: current status.** *Neurosurgery* 1985;16:11–16
9. Guglielmi G, Vinuela F, Dion J, Duckwiler G. **Electrothrombosis of saccular aneurysms via endovascular approach: preliminary clinical experience.** *J Neurosurg* 1991;75:8–14
10. Fox AJ, Vinuela F, Peltz DK, et al. **Use of detachable balloons for proximal artery occlusion in the treatment of unclippable cerebral aneurysms.** *J Neurosurg* 1987;66:40–44
11. Spetzler RF, Fukushima T, Martin N, Zabramski J. **Petrous carotid-to-intradural carotid saphenous vein graft for intracavernous giant aneurysm, tumor and occlusive cerebrovascular disease.** *J Neurosurg* 1990;73:496–501
12. Mathis JM, Barr JD, Jungreis CA, et al. **Temporary balloon test occlusion of the internal carotid artery: experience in 500 cases.** *AJNR Am J Neuroradiol* 1995;16:749–754
13. Standard S, Ahuja A, Guterman L, et al. **Balloon test occlusion of the internal carotid artery with hypotensive challenge.** *AJNR Am J Neuroradiol* 1995;16:1453–1458
14. Eckard D, Purdy P, Bonte F. **Temporary balloon occlusion of the carotid artery combined with brain blood flow imaging as a test to predict tolerance to permanent carotid sacrifice.** *AJNR Am J Neuroradiol* 1992;13:1565–1569
15. Giller CA, Mathews D, Walker B, Purdy P, Roseland AM. **Prediction of tolerance to carotid artery occlusion using transcranial Doppler ultrasound.** *J Neurosurg* 1994;81:15–19
16. Morioka T, Matsushima T, Fujii K, Fukui M, Hasuo K, Hisashi K. **Balloon test occlusion of the internal carotid artery with monitoring of compressed spectral arrays (CSAs) of electroencephalography.** *Acta Neurochir* 1989;101:29–34
17. Rordorf G, Koroshetz WJ, Copen WA, et al. **Diffusion- and perfusion-weighted imaging in vasospasm after subarachnoid hemorrhage.** *Stroke* 1999;30:599–605
18. Rordorf G, Koroshetz WJ, Copen WA, et al. **Regional ischemia and ischemic injury in patients with acute middle cerebral artery stroke as defined by early diffusion-weighted and perfusion-weighted MRI.** *Stroke* 1998;29:939–943
19. Østergaard L, Johannsen P, Host Poulsen P, et al. **Measurement of cerebral blood flow by dynamic bolus tracking: comparison with PET in humans.** *J Cerebral Blood Flow Metab* 1997;17: S442
20. Neumann-Haefelin T, Wittsack HJ, Wenserski F, et al. **Diffusion- and perfusion-weighted MRI: the DWI/PWI mismatch region in acute stroke.** *Stroke* 1999;30:1591–1597
21. Cutrer FM, Sorensen AG, Weisskoff RM, et al. **Perfusion-weighted imaging defects during spontaneous migrainous aura.** *Ann Neurol* 1998;43:25–31
22. Fisher M, Albers GW. **Applications of diffusion-perfusion magnetic resonance imaging in acute ischemic stroke.** *Neurology* 1992;52:1750–1756
23. Lythgoe DJ, Østergaard L, Williams SCR, et al. **Quantitative perfusion imaging in carotid artery stenosis using dynamic susceptibility contrast-enhanced magnetic resonance imaging.** *Magn Res Imaging* 2000;18:1–11
24. Rosen BR, Belliveau JW, Buchbinder BR, et al. **Contrast agents and cerebral hemodynamics.** *Magn Res Med* 1991;19:285–292
25. Röther J, Gückel F, Neff W, Schwartz A, Hennerici M. **Assessment of regional cerebral blood volume in acute human stroke**

**by use of single-slice dynamic susceptibility contrast-enhanced magnetic resonance imaging.** *Stroke* 1996;27:1088–1093
26. Schreiber WG, Guckel F, Stritzke P, Schmiedek P, Schwartz A, Brix G. **Cerebral blood flow and vascular reserve capacity: estimation by dynamic magnetic resonance imaging.** *J Cereb Blood Flow Metab* 1998;18:1143–1156
27. Belliveau JW, Rosen BR, Kantor HL, et al. **Functional cerebral imaging by susceptibility-contrast NMR.** *Magn Reson Med* 1990;14:538–546
28. Gückel F, Brix G, Rempp K, Deimling M, Röther J, Georgi M. **Assessment of cerebral blood volume with dynamic susceptibility contrast-enhanced gradient-echo imaging.** *J Comput Assist Tomogr* 1994;18:344–351
29. Fisel CR, Ackerman JL, Buxton RB, et al. **MR contrast due to microscopically heterogeneous magnetic susceptibility: numerical simulation and application to cerebral physiology.** *Magn Res Med* 1991;17:336–347
30. Edelman RR, Mattle HP, Atkinson DJ, et al. **Cerebral blood flow: assessment with dynamic contrast-enhanced T2-weighted MR imaging at 1.5 T.** *Radiology* 1990;176:211–220
31. Fukunaga A, Uchida K, Hashimoto J, Kawase T. **Neuropsychological evaluation and cerebral blood flow study of 30 patients with unruptured cerebral aneurysms before and after surgery.** *Surg Neurol* 1999;51:132–139
32. Levine RL, Rozental JM, Nickles RJ. **Blood flow asymmetry in carotid occlusive disease.** *Angiology* 1992;43:100–109
33. Dahl A, Russell D, Nyberg-Hansen R, Rootwelt K, Bakke SJ. **Cerebral vasoreactivity in unilateral carotid artery disease—a comparison of blood flow velocity and regional cerebral blood flow measurements.** *Stroke* 1994;25:62–66
34. Gibbs JM, Wise RJ, Leenders KL, Jones T. **Evaluation of cerebral perfusion reserve in patients with carotid-artery occlusion.** *Lancet* 1984;1:310–304
35. Sato O, Kamitani H. **Giant aneurysm of the middle cerebral artery: angiographic analysis of blood flow.** *Surg Neurol* 1975; 4:27–31
36. Strother CM. **In vitro study of hemodynamics in a giant saccular aneurysm model: influence of flow dynamics in the parent vessel and effects of coil embolization.** *Neuroradiology.* 1995;37:159–161
37. Gilsbach JM, Harders AG. **Microvascular and transcranial Doppler sonograph evaluation of cerebral aneurysm flow pattern.** *Neurol Res* 1989;11:41–48
38. Lawton MT, Hamilton M, Morcos J, Spetzler RF. **Revascularization and aneurysm surgery: current techniques, indications, and outcome.** *Neurosurgery* 1996;38:83–94
39. Sen C, Segal HD. **Is carotid artery reconstruction mandatory?** *Clin Neurosurg* 1994;42:135–153
40. Cantore G, Santoro A. **Treatment of aneurysms unsuitable for clipping or endovascular therapy.** *J Neurosurg Sci* 1998;42: 71–75
41. Santoro A, Guidetti G, Dazzi M, Cantore G. **Long saphenous-vein graft for extracranial and intracranial internal carotid artery aneurysms amenable neither to clipping nor to endovascular treatment.** *J Neurosurg Sci* 1999;43:237–251
42. Caramia F, Huang Z, Hamberg LM, et al. **Mismatch between cerebral blood volume and flow index during transient focal ischemia studied with MRI and Gd-BOPTA.** *Magn Reson Imaging* 1998;16:97–103